

## Article

# New Year Fireworks Influence on Air Quality in Case of Stagnant Foggy Conditions

Audrė Kalinauskaitė , Lina Davulienė , Julija Pauraite , Agnė Minderytė  and Steigvilė Byčenkienė \* 

SRI Center for Physical Sciences and Technology (FTMC), Department of Environmental Research, Saulėtekio Ave. 3, LT-10257 Vilnius, Lithuania; audre.kalinauskaitė@ftmc.lt (A.K.); lina.davulienė@ftmc.lt (L.D.); julija.pauraite@ftmc.lt (J.P.)

\* Correspondence: steigvile.bycenkiene@ftmc.lt

**Abstract:** Urban science plays a pivotal role in understanding the complex interactions between fireworks, air quality, and urban environments. Dense firework smoke worsens air quality and poses a health hazard to the public. In this study, we show a situation where extremely foggy meteorological conditions coincided with intense anthropogenic emissions, including fireworks, in an urban area. For the first time, the chemical composition and sources of non-refractory submicron aerosol (NR-PM<sub>1</sub>) in outdoor and indoor air were characterized in Vilnius (Lithuania) using an aerosol chemical speciation monitor (ACSM) and Positive Matrix Factorization for the period before the fireworks, on New Year's Eve, and after the fireworks in 2020/2021; thus, typical changes were assessed. Due to stagnant weather conditions and increased traffic, the highest concentrations of black carbon (BC) (13.8 μg/m<sup>3</sup>) were observed before the fireworks display. The contribution of organic (Org) fraction to the total NR-PM<sub>1</sub> mass concentration, in the comparison of the values of a typical night and New Year's Eve (from 9 p.m. to 6 a.m.), increased from 43% to 70% and from 47% to 60% in outdoor and indoor air, respectively. Biomass-burning organic aerosol (BBOA, 48% (44%)) and hydrocarbon-like organic aerosol (HOA, 35% (21%)) dominated the organic fraction indoors and outdoors, respectively. HOA was likely linked to increased traffic during the event, while BBOA may have been related to domestic heating and fireworks.

**Keywords:** air pollution; urban background site; organic aerosol; fireworks; PMF; source apportionment; indoor



**Citation:** Kalinauskaitė, A.; Davulienė, L.; Pauraite, J.; Minderytė, A.; Byčenkienė, S. New Year Fireworks Influence on Air Quality in Case of Stagnant Foggy Conditions.

*Urban Sci.* **2024**, *8*, 54. <https://doi.org/10.3390/urbansci8020054>

Received: 28 March 2024

Revised: 11 May 2024

Accepted: 16 May 2024

Published: 20 May 2024



**Copyright:** © 2024 by the authors. Licensee MDPI, Basel, Switzerland. This article is an open access article distributed under the terms and conditions of the Creative Commons Attribution (CC BY) license (<https://creativecommons.org/licenses/by/4.0/>).

## 1. Introduction

Despite their cultural significance, fireworks pose environmental challenges in densely populated urban environments. Studies of the effects of fireworks on air quality have intensified in recent decades as awareness of the impact of air pollution on human health has grown [1–3]. Unlike other anthropogenic sources of air pollution, fireworks are mostly used on spatial public or private occasions to emphasize the festivity of a moment and are an event appreciated by a large part of the population. Fireworks can last from a few minutes to half an hour or longer and contribute significantly to air pollution. Health complications attributed to fireworks emissions include headaches and respiratory and/or cardiovascular problems [4–7]. Therefore, the content and use of fireworks are becoming the subject of regulation by legislation [8,9]. Since fireworks pollution is a combination of primary (smoke) and secondary particles resulting from additional chemical reactions, the effects on indoor air quality are due to a combination of both [10]. Indoor air pollution is the main problem for people living in urban areas because they spend almost 90% of their daily time indoors [11]. Furthermore, the World Health Organization revealed that indoor air pollution took the lives of 3.8 million people exposed to air pollution [12]. Therefore, although many studies have focused on outdoor air quality, to date, there has been little research that examines long-term trends in indoor and outdoor air quality simultaneously.

An overview of the largest fireworks events in the world is provided in a paper by Hoyos, 2020 [7]. Air pollutants from fireworks generally consist of particulate matter (PM), black carbon (BC), SO<sub>2</sub>, CO, and NO<sub>x</sub> [1]. Metal salts used as colorants in fireworks are released into the atmosphere in large quantities and are included in PM<sub>2.5</sub> [9,13]. Each firework display is a unique event in terms of the color composition, and therefore, the ratios of the metals used for coloring are also unique [13]. During a fireworks display, concentrations of air pollutants can be several times higher compared to background levels [14–17], especially when the fireworks activities occur over a large area and over a long period of time, as observed in previous studies [18,19]. An hour after the fireworks, an increase in the hourly average concentrations of PM<sub>2.5</sub> and PM<sub>10</sub> was observed, although no parallel increase in BC was detected [7]. However, some authors concede that fireworks can also lead to increased BC concentrations [20–22] and PM mass concentrations which are dominated by submicron particles [23,24]. An increase in fine particle mass concentration during a fireworks display was observed for up to half an hour after the peak of the fireworks show [25], and the number concentration of aerosol particles in accumulation mode was observed for up to three hours, along with increases in PM<sub>2.5</sub> and PM<sub>10</sub> mass concentrations [26].

The duration of increased air pollution from fireworks can range from a few hours to several days or weeks, depending on meteorological conditions and the dynamic parameters of the PM in the atmosphere [27,28]. According to Hoyos et al. (2020) [7], the change in PM concentration from a sharp increase to a standstill depends on meteorological conditions such as wind speed, wind direction, and atmospheric stability, as well as on the location of the monitoring station, which depends on local and regional geographical features.

Positive Matrix Factorization (PMF) has been used extensively to perform source apportionment from filter-based and online measurements [29,30]. Real-time aerosol particle measurements can provide chemical compositions, mixing states, and apportion sources, and they are beneficial for the short-term analysis of air pollution episodes [31–33]. The application of PMF and multiple linear regression showed that the contribution of fireworks to the total PM<sub>10</sub> mass was about 50% (33.6 µg/m<sup>3</sup>), organic and elemental carbon were 12% and 4%, respectively, and metals accounted for less than 2% [34,35].

In this study, we aimed to investigate the contribution of fireworks to submicron aerosol particles. The aim of the present study was to characterize the chemical composition of PM<sub>1</sub> associated with New Year's Eve fireworks in a European city (Vilnius, the capital of Lithuania, with ~600,000 inhabitants). In order to evaluate indoor and outdoor air quality variations caused by fireworks, the data from New Year's Eve were compared with the control period (typical winter days).

## 2. Materials and Methods

### 2.1. Sampling Site and Measurement Periods

The chemical composition and sources of PM<sub>1</sub> were analyzed indoors and outdoors in the low-energy (Class B) building of the SRI Center for Physical Sciences and Technology (FTMC) [36] at 54.72° N, 25.32° E in Vilnius (in the urban background site), Lithuania, from 18 December 2020 to 15 January 2021 (Figure 1). The office is located on the second floor of the building, and indoor aerosol samples were collected approximately 1 m above the floor of the room. The intake air was cleaned with a three-stage filtration system (G4-F7-F9). According to the standard DIN EN ISO 16890 [37], the filtration efficiency of G4 corresponds to 70% for coarse particles. The second filter (F7) achieved an effective removal efficiency of 65–95% for PM<sub>2.5</sub> and 50–56% for PM<sub>1</sub>.

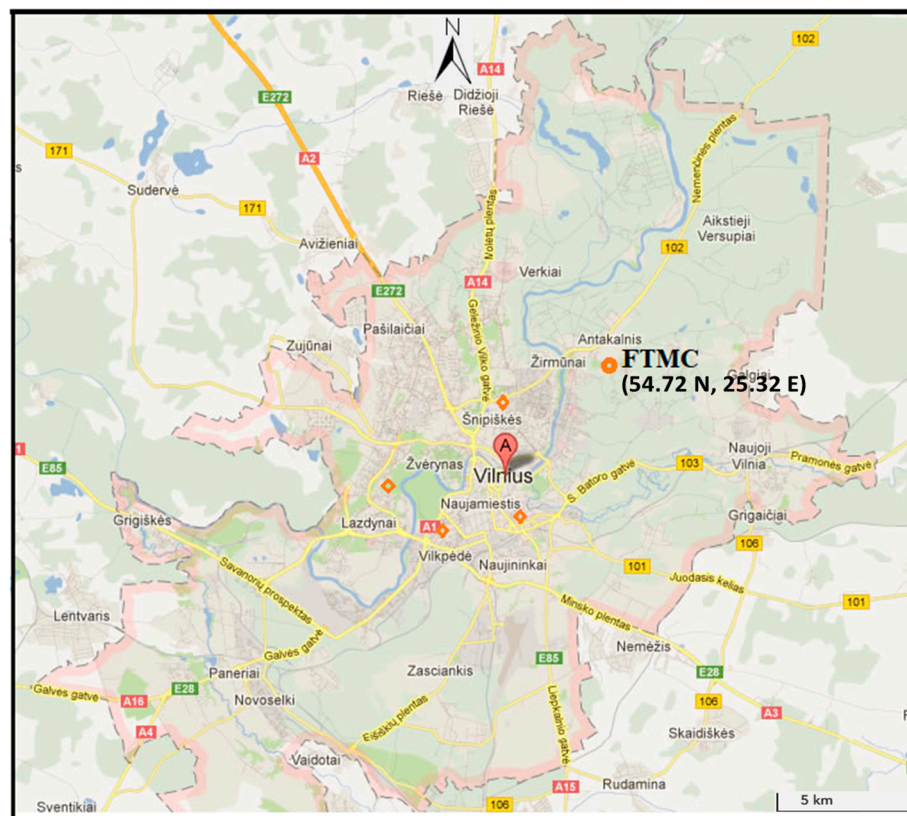


**Figure 1.** Location of sampling sites (orange circle—FTMC, orange diamonds—national air quality monitoring stations). Source: [www.maps.lt](http://www.maps.lt), accessed on 1 July 2021.

## 2.2. Instrumentation, Data Sources, and Models

An aerosol chemical speciation monitor (ACSM, Aerodyne Research, Inc., Billerica, MA, USA) was used to measure the chemical composition of non-refractory submicron aerosol (NR-PM<sub>1</sub>). Inside the instrument, aerosol particles are focused by aerodynamic lenses and travel under a high vacuum onto a heated porous tungsten surface of 600 °C. Non-refractory species (NH<sub>4</sub><sup>+</sup>, NO<sub>3</sub><sup>-</sup>, SO<sub>4</sub><sup>2-</sup>, Cl<sup>-</sup>, and organic matter (Org)) are flash-vaporized and ionized by electron impact at 70 eV. Molecular fragments were subsequently detected by a quadrupole mass spectrometer. The time resolution of a 30 min interval was used. The collection efficiency of 1 was applied to avoid the overestimation of the PM<sub>1</sub> concentration compared to PM<sub>2.5</sub> data. The 30 min ACSM detection limits were 0.2, 0.08, and 0.05 µg/m<sup>3</sup> for organic matter, nitrate, and sulfate, respectively. The ACSM sampling line was equipped with a critical aperture of 100 µm diameter and an aerodynamic lens system in the ACSM inlet designed for PM<sub>1</sub> sampling. The flow rate through the critical aperture varied between 80 and 150 cm<sup>3</sup> min<sup>-1</sup>. There was no additional cut-off impactor in the ACSM sampling line.

An aethalometer (A Magee Scientific, Model AE31 Spectrum, manufactured by Optotek, Slovenia) was used for the simultaneous indoor and outdoor measurement of black carbon mass concentration. The optical transmission of carbonaceous aerosol particles was measured at 7 wavelengths (370, 470, 520, 590, 660, 880, and 950 nm). The measurements at 880 nm were used to calculate the equivalent BC concentration using the wavelength-specific attenuation cross-section (16.6 m<sup>2</sup> g<sup>-1</sup>) specified by the manufacturer. The correction was applied to reduce some systematic errors, including filter loading and multiple scattering effects of the aethalometer data. The measured data were recorded at 5 min intervals, and the flow rate was 4.9 L min<sup>-1</sup>. The aethalometer was equipped with an additional impactor that removed particles with an aerodynamic diameter greater than 2.5 µm.

BC source apportionment was determined using the aethalometer model proposed by Sandradewi et al., 2008 [38]. Briefly, this method uses the absorption Angstrom exponent (AAE) with wavelengths of 470 and 880 nm. Based on a previous study of BC in Vilnius by Minderytė et al., 2022 [39], AAE = 0.9 indicates local fossil fuel combustion emissions, while AAE = 2.2 corresponds to BC originating from local wood burning.

The outdoor aerosol inlet of the online aerosol measurement equipment (an aethalometer and aerosol chemical speciation monitor) was approximately 5 m above the ground, while the indoor aerosol samples were taken approximately 1 m above the floor of the room. An automatic valve control was used to switch sampling between indoor and outdoor inlets with a time resolution of 30 min. The PM<sub>1</sub> assessment by the ACSM is defined as  $PM_1 = \text{Org} + [NH_4^+] + [NO_3^-] + [SO_4^{2-}] + [Cl^-] + BC$  [40]. The BC value was taken from measurements of the AE31 aethalometer.

This study is part of a larger study which took measurements during the heating season from 15 October 2020 to 8 February 2021, presented in Garbarienė et al., 2022 [41]. The detailed description of the experimental setup can be found there (2.1. Measurement location and study design [41]). Meteorological data were obtained from the National Oceanic and Atmospheric Administration (NOAA) Air Resources Laboratory (ARL) data archives, Lithuanian Hydrometeorological Service data archives (via API access), and Germany's National Meteorological Service, the Deutscher Wetterdienst (DWD). The data are provided in the UTC+0 time zone.

PM<sub>2.5</sub> and PM<sub>10</sub> mass concentrations, NO<sub>2</sub>, CO, and meteorological parameters were collected at the Environmental Protection Agency (EPA) monitoring stations: Old Town, Žirmūnai, Lazdynai, and Savanorių ave. Hourly average values were calculated from the first to the last minute (e.g., 00:01:00–01:00:00) of the hour.

We used the thermodynamic equilibrium model ISORROPIA-II [39] to evaluate the sodium mass concentration. This method calculates equilibrium partitioning based on the total concentration of the different species. ISORROPIA-II sets up a system of equilibrium equations and solves them to reach the equilibrium state using the chemical potential method [42].

The backward trajectories of the air parcels were calculated with the National Oceanic and Atmospheric Administration (NOAA) Hybrid Single-Particle Lagrangian Integrated Trajectory (HYSPLIT) model [43,44] using the Global Data Assimilation System (GDAS) with 1° resolution. Single-day backward trajectories for 24 h ending at 00:00 UTC+2 on 1 January 2021 were calculated for the endpoint at the FTMC measurement site at altitudes of 50, 500, and 1000 m above sea level.

### 3. Results and Discussion

As firework aerosols tend to accumulate in large amounts in a very short period of time, they cause a hazard to environmental and human health. In contrast to previous studies focusing mainly on the concentration and composition of PM<sub>2.5</sub> and PM<sub>10</sub> altered by fireworks, this study aimed to investigate the changes in organic aerosol and black carbon in PM<sub>1</sub> outdoors and indoors before and after New Year's Eve fireworks under stagnant foggy conditions. The determination of the composition of the organic aerosol fraction and BC in the fine mode of particulate matter is necessary to provide information on their ability to penetrate indoors and their higher potential to settle in the deepest parts of the human respiratory system.

#### 3.1. Meteorological Conditions

In the period of 18th and 25th December 2020, the weather was influenced by a high-pressure system over northern Europe and cyclones from the west. Weather conditions were mild, with the average air temperature reaching 1.26 °C, wind speed reaching up to 3.61 m/s, relatively high pressure (2018.16 hPa), and ~95% relative humidity. The amount of precipitation was 11.9 mm for this period.

From the second day of Christmas to the first day of New Year, the influence of low-pressure systems from the west (Figure 2a) and southeast and short periods of high-pressure fields over northern Europe resulted in cloudy, foggy weather and light snow and sleet in Vilnius. On average, the air temperature reached just 0.76 °C, and windiness reached 4 m/s. However, the atmospheric pressure and relative humidity were lower compared to the previously studied period, reaching, on average, 1008.8 hPa and ~91%, respectively.

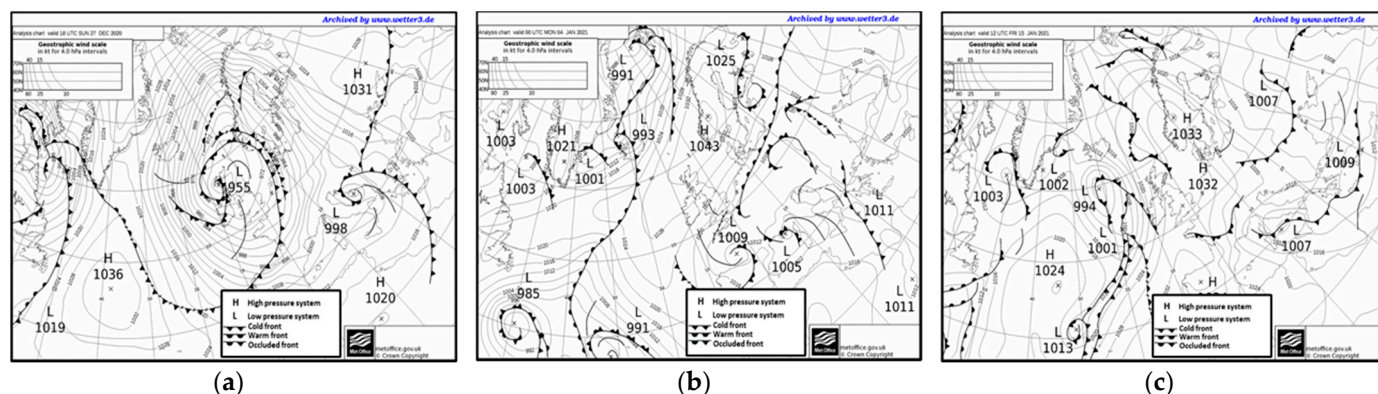


**Figure 2.** Examples of various synoptic situations from 18 December 2020 to 8 January 2021: (a) 27 December 2020, 18 UTC; (b) 4 January 2021, 00 UTC; (c) 15 January 2021 12 UTC.

Furthermore, between 2nd and 8th January 2021, the higher-pressure system (Figure 2b) was replaced by a low-pressure system from the south, and later, another cyclone moved from the south. Such dynamics of pressure systems over northern Europe increased the amount of precipitation (16.5 mm) and mean relative humidity (~97%) in Lithuania compared to the aforementioned period. Meanwhile, the average air temperature was just below 0 (−0.36 °C), and windiness declined to 2.12 m/s—1.9 times weaker than the previous episode. However, the atmospheric pressure during the whole period was quite high and reached 1017 hPa.

In this period, the weather conditions in Vilnius were determined by anticyclones (Figure 2c) and a cyclone from the northwest which passed through Lithuania in the middle of this period. The higher atmospheric pressure during this episode resulted in a lower average air temperature (−4.92 °C), which dropped sharply towards the end of the episode, reaching a minimum of −18.5 °C. All other meteorological parameters, except wind speed (the mean value was 2.88 m/s), reached lower average values in comparison with the earlier studied period. The average atmospheric pressure declined by 4 hPa to 1013.3 hPa, and the air relative humidity decreased by 7% up to 90.15%. Meanwhile, the amount of precipitation was 2.6 times lower than in the previous period, reaching 6.3 mm.

The average air temperature during the entire measurement campaign was −0.8 °C (ranging from −18.5 °C to 6.7 °C), while the relative humidity reached an average of 93% (max: 100%; min: 67%) and the total precipitation was 44.4 mm (SD: 0.2 mm). The average wind speed was 3.2 m/s and varied between 0.4 m/s and 8.8 m/s, while the atmospheric pressure reached 1014.5 hPa on average and varied between 994.3 hPa and 1030 hPa.

The average night-time meteorological parameters (9 p.m.–6 a.m. UTC+0) were close to those obtained for the entire study period. The average nocturnal air temperature during the entire measurement campaign was −0.9 °C (ranging from −18.5 °C to 5.3 °C), while the relative humidity was 94% (max: 100%, min: 76%) and the total precipitation was 14.2 mm (SD: 0.1 mm). The average wind speed was 3.1 m/s and varied between 0.8 m/s and 8.2 m/s, and the atmospheric pressure reached 1014.5 hPa and varied between 996.3 hPa and 1030.0 hPa.

Meteorological conditions were an important factor strongly influencing the concentration of PM on New Year's Eve and during fireworks displays. In Vilnius, the maximum temperature on December 31 reached +3.2 °C, and the average wind speed during the day was about 1.54 m/s (Figure 3a). The relative humidity was high, at 98% on average,

and the atmospheric pressure was low, at 1009.7 hPa. From 8:00 a.m. on 31 December to 6:00 a.m. on 1 January, foggy and cloudy conditions prevailed in Vilnius County without significant precipitation.

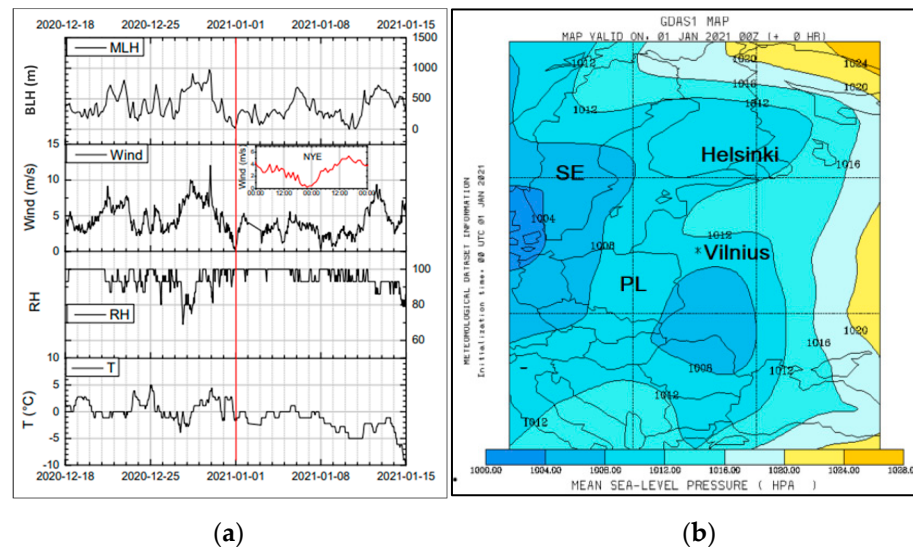


**Figure 3.** Meteorological situation: (a) Meteorological parameters (mixing height, wind speed, relative humidity, air temperature) at Vilnius Airport station from 18 December 2020 to 15 January 2021 and (b) mean sea level pressure distribution over the region on 1 January at 00:00 UTC.

On 31st of December and 1st of January, the weather was driven by a relatively higher-pressure area with a low pressure gradient (Figures 3b and 4a,b).

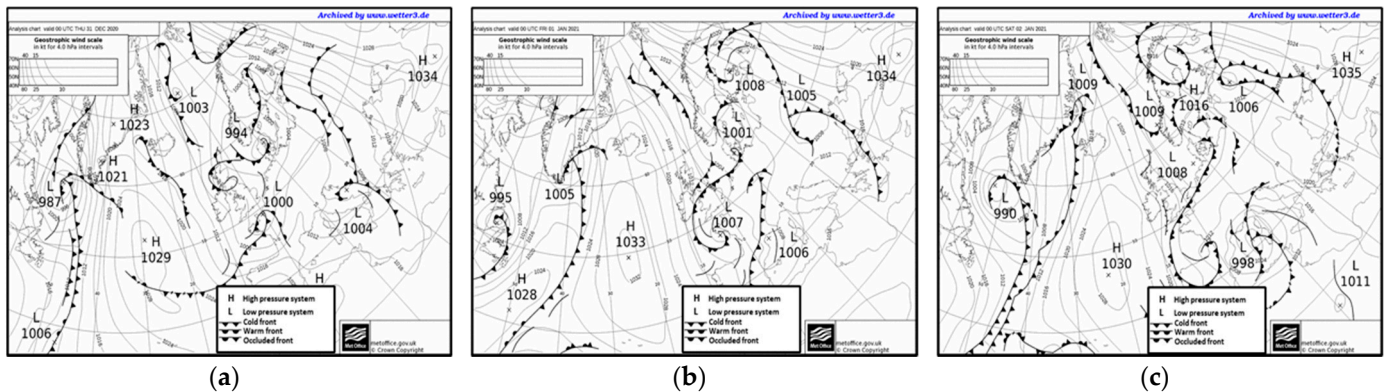


**Figure 4.** Synoptic maps for New Year's Eve (a), New Year's night (b), and 2 January (c).

These conditions led to the prevailing foggy and misty weather in Vilnius. The average air temperature during the night of 31 December–1 January was  $-0.8\text{ }^{\circ}\text{C}$  (ranging from  $-1.7\text{ }^{\circ}\text{C}$  to  $0\text{ }^{\circ}\text{C}$ ), i.e., it was close to the average night air temperature during the whole measurement campaign. Meanwhile, the average relative humidity was 99.7%, 5% higher than during the whole measurement period (Figure 3a). The atmospheric pressure reached 1010.5 hPa (with variations between 1009.2 and 1011.8 hPa). Even though foggy conditions prevailed in Vilnius district during the night of 31st December–1st January, since a southern cyclone with a warm front ahead approached Lithuania from the southeast early on New Year's morning (Figure 4b), snow and rain precipitated a little at that time and in the afternoon on January 1. The total precipitation on New Year's night was only 1.1 mm, while on the nights during the whole measurement period, the total precipitation was almost 13 times higher, reaching 14.2 mm. On New Year's Eve, the wind was changeable, while on New Year's Day, northwest and northeast winds prevailed at the measurement site (Figure 5a).

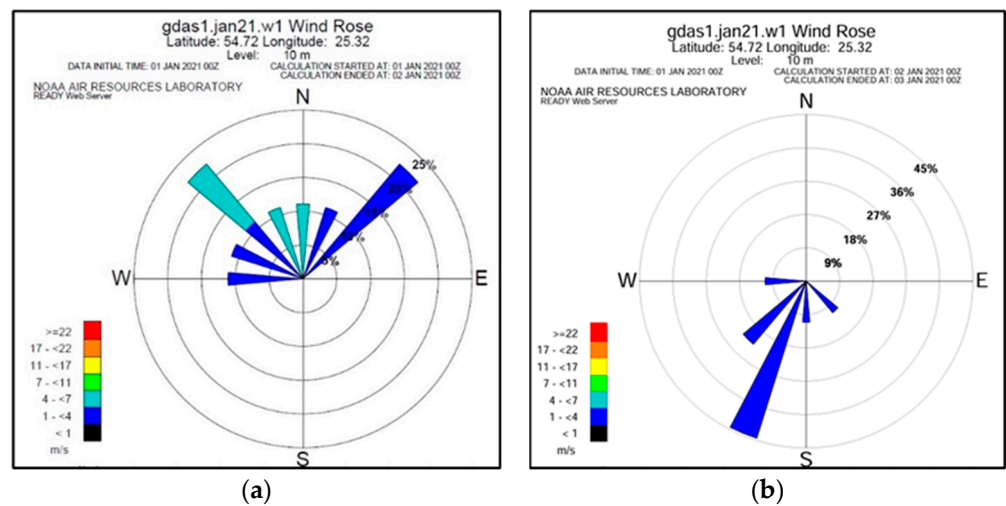


Figure 5. Windrose for 1 January (a) and 2 January 2021 (b).

The average wind speed was 1.3 m/s (ranging from 0.9 to 1.9 m/s), 2.3 times lower than the average wind speed during the entire campaign. On 2nd of January, the weather conditions were relatively similar to the two previous days. Even though low-pressure systems prevailed in northern Europe, the weather in Lithuania was still influenced by relatively higher atmospheric pressure (~1018 hPa in average) with a low pressure gradient (Figure 4c). The weather conditions were mostly foggy, except for short snow showers in the morning, and the relative humidity (average 97.4%) remained similar to the previous days; however, on 2nd of January, the air temperature was a bit lower (average ~−1.37 °C) and west–southwest winds prevailed during the day, which changed to a southeast wind in the late evening (Figure 5b). Windiness strengthened up to 2.1 m/s on average.

In order to verify whether thermal inversion had formed on New Year’s night, a vertical air temperature profile was used (Figure 6).

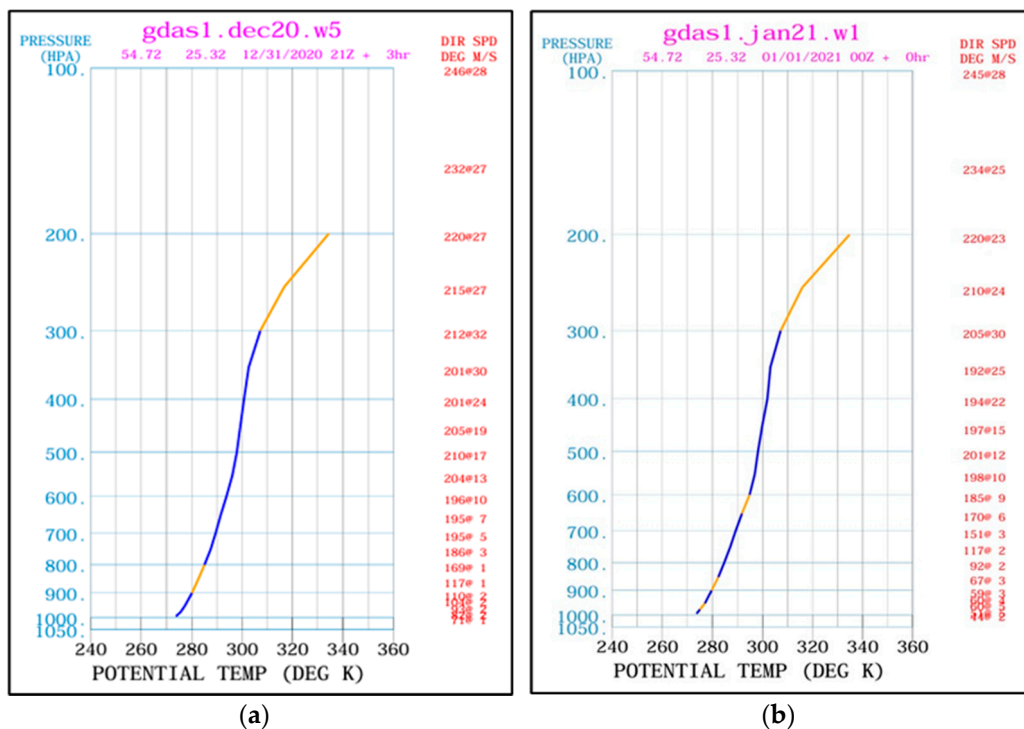
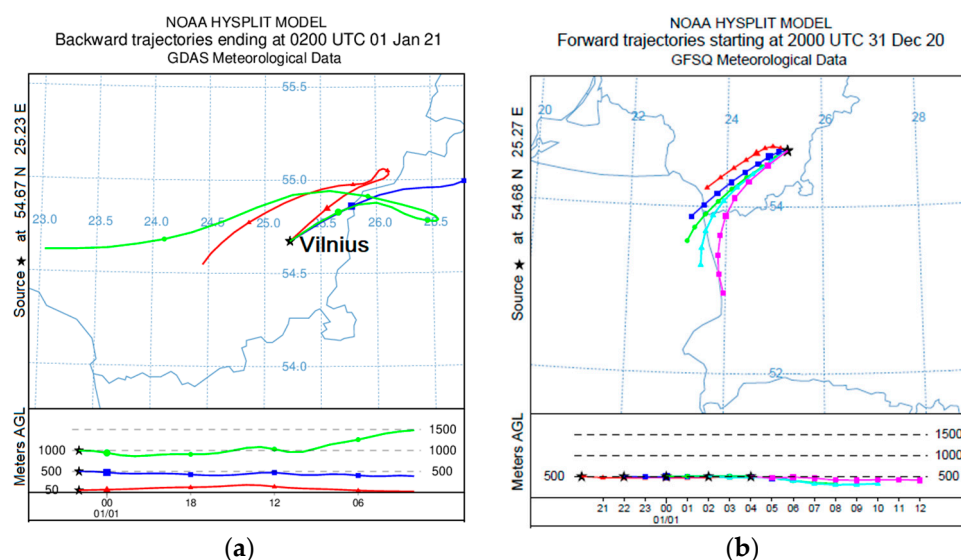


Figure 6. Vertical air potential temperature profile for New Year’s Eve (a) and night (b).

The orange segments of the theta line denote the critical inversions. These segments met the criteria, defined by Heffter (1983) [45], of a critical inversion which capped vertical mixing in the planetary boundary layer. Meanwhile, the blue line in the figure is the potential temperature along the moist adiabat. According to Figure 6a, the height of the inversion layer spanned between 900 and 800 hPa on New Year's Eve. On the night of January 1, several layers of thermal inversion formed, with heights between more than 900 hPa and 600 hPa (Figure 6b). Since we aimed to see the inversion in the mixing layer, we did not discuss the thermal inversion above the 500 hPa level. The theta lines appeared to slope evenly, which coincided with a state of atmospheric stability on New Year's Eve. Such stable atmospheric conditions and thermal inversion worsened air quality in the urban background site in Vilnius, as was also observed in another study by Ji et al., 2012 [46]. The stable stratification of the atmosphere usually forms during inversion, and, consequently, the development of the planetary boundary layer (PBL) is disrupted: atmospheric convection and turbulence are attenuated, allowing particles and pollutants to accumulate beneath the inversion layer [47].

During this period, the planetary boundary layer height (BLH) varied from 99–180 m on the morning of 31 December to 327–343 m on January 1. According to the Pasqual stability classes, the atmosphere varied between neutral (Class D), slightly stable (Class E), and moderately stable (Class F) conditions. Considering the stability of the atmosphere, relatively low air temperature, low wind speed, and foggy status, the meteorological conditions were favorable for the accumulation of particulate matter in the atmosphere on the eve and night of New Year. Short trajectories indicate slow-moving air masses that could accumulate pollutants along their route (Figure 7).



**Figure 7.** HYSPLYT air mass trajectories: (a) backward trajectories for 24 h ending at 00:00 on 1 January 2021; (b) forward trajectories starting every 2 h from 20:00 on 31 December 2020.

As shown in Figure 7, the air mass backward trajectory that flew the lowest (red color) only went through the territory of Lithuania. Meanwhile, the other two trajectories also moved over the western area of Belarus (Figure 7a). During the cold season, home heating with biomass (firewood, biofuel), intensive traffic in larger cities, and New Year's fireworks, under favorable meteorological conditions for the accumulation of air pollutants, made it possible for these short and slowly moving air masses to accumulate atmospheric aerosol particles on their way to the receptor point in Vilnius. Meanwhile, the air mass trajectories moving slowly from Vilnius to the southwest (Figure 7b) could have potentially carried away some of the air pollutants, taking into account the mass concentrations of aerosol particles that started to fall after New Year's Eve (Figure 8).

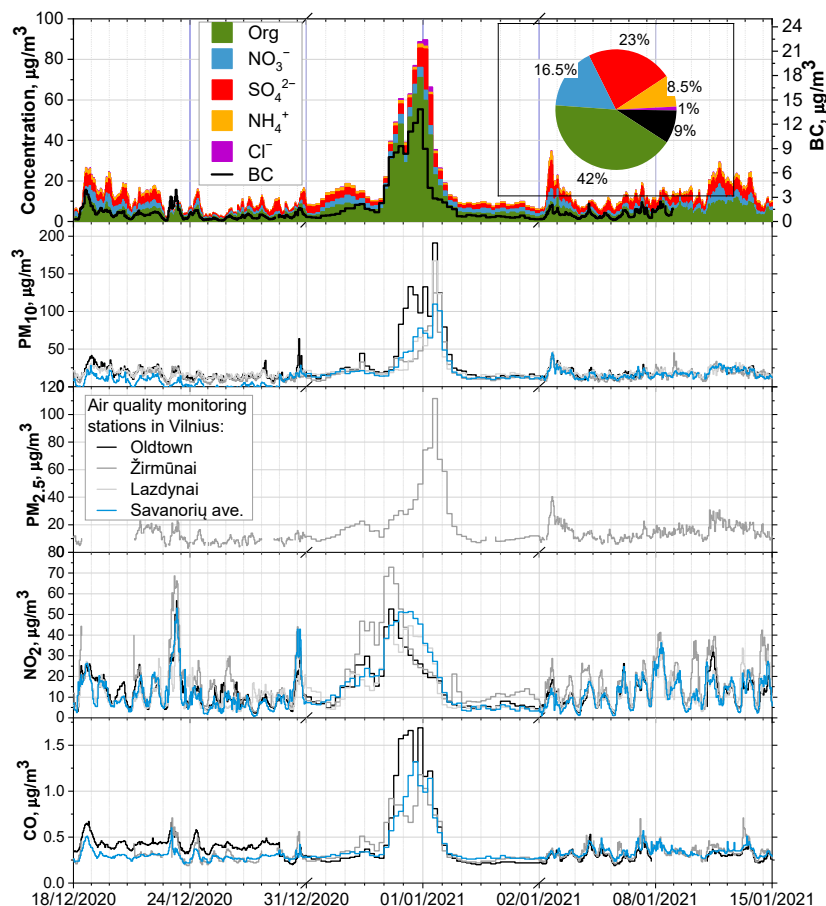


**Figure 8.** Time series of organics (Org), sulfate ( $\text{SO}_4^{2-}$ ), ammonium ( $\text{NH}_4^+$ ), nitrate ( $\text{NO}_3^-$ ), and chlorine ( $\text{Cl}^-$ ) measured by an ACSM with a 30 min resolution and BC measured by an aethalometer outdoors before/after and during the New Year at the FTMC measurement in Vilnius during this study and mean concentrations of  $\text{PM}_{2.5}$ ,  $\text{PM}_{10}$ ,  $\text{NO}_2$ , and CO observed across the EPA sites (Old Town, Žirmūnai, Lazdynai, and Savanorių ave.) covering the Vilnius area. The inset pie chart shows the relative contribution over the whole period.

However, similar meteorological conditions prevailed on other observed days (e.g., 5 and 6 January), and apart from New Year's Eve, no other significant increase in aerosol mass concentration was observed. Thus, meteorology played an important role in the accumulation of pollutants, but additional sources of pollution were present on New Year's Eve.

Fog is known for its scavenging effect in the atmospheric boundary layer considering air pollution. Such an effect has been observed in various scientific studies [48–50]. Meanwhile, in our case study, an increase in the air pollution level before and during New Year's night was observed while foggy conditions remained. However, the stable atmospheric conditions and low wind speed might have had a significant impact on the elevated concentrations of  $\text{PM}_1$  components. The mechanism of the impact of a lower BLH on concentrations of atmospheric aerosol particles has been explained in other studies [49,51], which mainly state that a lower BLH slows down the diffusion of pollutants that, consequently, leads to the development of air pollution.

### 3.2. Variation of Air Quality and PM Composition

The time series of outdoor  $\text{PM}_1$  species and their relative contribution to  $\text{PM}_1$  components were analyzed along with some other air quality parameters during the study period from 18 December 2020 to 15 January 2021. The highest levels of mass concentrations of air pollutants were observed on New Year's Eve from 31 December 2020 to 1 January

2021 (between 9:00 p.m. and 6:00 a.m.) compared to the analyzed period (Figures 8 and 9, Table 1). Pirker et al., 2022 [52] also observed a similar tendency. Therefore, the last day of 2020 and the first day of 2021 were plotted at higher resolutions to track the variation in the concentration levels of PM<sub>1</sub> components during New Year’s Eve (Figure 8).

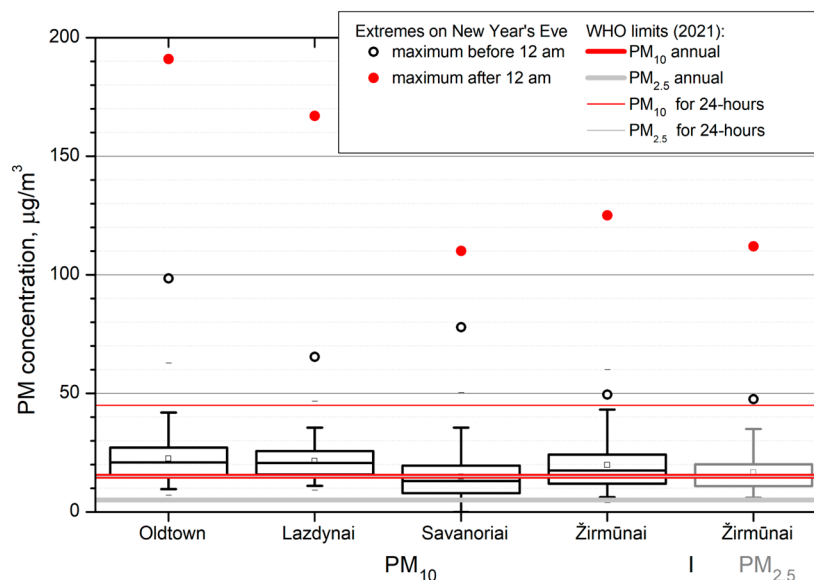


**Figure 9.** Box-and-whisker plot for the control period and the maximum PM<sub>10</sub> and PM<sub>2.5</sub> levels during New Year’s Eve after 12 a.m. (red cycles) along with the PM<sub>10</sub> and PM<sub>2.5</sub> mass concentration limits established by the WHO. Whiskers: the 1st and 99th percentiles (error bars), quartiles Q1 and Q3 (box), median (horizontal line), and mean (square).

**Table 1.** Descriptive statistics of concentration values (µg/m<sup>3</sup>) for the control period (18 December 2021–15 January 2022) and New Year’s Eve.

FTMC site	Control Period without New Year’s Eve (9 p.m.–6 a.m.)				New Year’s Eve (9 p.m.–6 a.m.)			Factor, NYmax/P75
	Median	P75	P99	Max	11:30 p.m.	12:30 a.m.	Max	
Org	4.1	6.3	12	12	71	60	71	11.27
SO <sub>4</sub> <sup>2-</sup>	3.2	4.0	7.8	8.5	9.5	20	20	5.0
NO <sub>3</sub> <sup>-</sup>	1.7	2.6	7.5	8.2	5.0	5.0	5.0	1.92
NH <sub>4</sub> <sup>+</sup>	0.96	1.5	3.2	3.4	1.9	1.4	1.9	1.27
Cl <sup>-</sup>	0.05	0.10	0.44	0.46	1.3	3.2	3.2	32.0
BC	0.52	0.80	1.44	2.74	13.8	8.9	13.8	17.25
PM <sub>1</sub>	13.0	21.5	28.7	50.4	103	98.5	103	4.79
<b>EPA sites</b>								
PM <sub>2.5</sub> (Žirmūnai)	11.0	15.0	25.0	30.8	47.6	74	* 112	7.47
PM <sub>10</sub> (Žirmūnai)	11.8	15.9	26.0	33.8	49.5	74	* 125	7.86
PM <sub>10</sub> (Old Town)	15.9	20.7	38.9	41.6	98.5	133	* 191	9.23
PM <sub>10</sub> (Savanorių ave.)	12.0	17.3	30.0	30.8	77.9	71	* 110	6.36
PM <sub>10</sub> (Lazdynai)	16.9	21.3	31.8	33.4	65.4	54	* 167	7.84

\* Maximum values at EPA sites were observed at 2:30 a.m.

The outdoor concentrations of PM<sub>1</sub> components increased several times on New Year’s Eve (with a maximum at 12 a.m.) and reached the extreme values of the study period (Figure 8). However, only the Cl<sup>-</sup> and SO<sub>4</sub><sup>2-</sup> concentrations reached their maximum values immediately after midnight and could be attributed to the fireworks. The largest increase, by a factor of 21 compared to the 75th percentile (Q3) of the control period, was observed for Cl<sup>-</sup> (Table 1). A smaller but still extreme increase, with factors in the order of 8 to 10, was observed for BC and organics, while sulfate only increased by a factor of 3.5. The concentrations of nitrate and ammonia increased but remained below Q3 of the control period. The pie chart shows that the concentrations of PM<sub>1</sub> compounds occurred in the

following order during the typical period:  $\text{Org} > \text{SO}_4^{2-} > \text{NO}_3^- > \text{BC} > \text{NH}_4^+ > \text{Cl}^-$ . The first three components accounted for about 80% of the mass.

The mean values of CO and NO<sub>2</sub> in the Old Town area for the period of one-month measurements, covering the periods before and after New Year's Eve, were as follows (Figure 8): CO ( $0.35 \pm 0.09$ ) mg/m<sup>3</sup> and NO<sub>2</sub> ( $12.2 \pm 7.8$ ) µg/m<sup>3</sup>. The highest values were measured on New Year's Eve with 1.66 mg/m<sup>3</sup> for CO and 56.6 µg/m<sup>3</sup> for NO<sub>2</sub>. The increase in the concentration of CO coincided with the evening rush hour, as the concentration increased from 16:00 and lasted longer than the rush hour, reaching the highest values at 22:00 and 23:00 at Savanorių and Žirmūnų stations, which were 1.32 and 1.18 mg/m<sup>3</sup>, respectively (1.7 mg/m<sup>3</sup> in the Old town). NO<sub>2</sub> concentrations depend on traffic activity, and on December 31, the NO<sub>2</sub> levels increased during the day from the morning rush hour, peaked at 73 µg/m<sup>3</sup> at 16:00–17:00, and decreased at 18:00–20:00 and during the night. On the previous day, 30 December, the NO<sub>2</sub> concentrations were also elevated throughout the day, peaking at 35 µg/m<sup>3</sup> but declining rapidly after 18:00, as they did on 23 December, when the NO<sub>2</sub> concentrations reached 56.6 µg/m<sup>3</sup>. The maximum of daily NO<sub>2</sub> fluctuations is usually below 35 µg/m<sup>3</sup> at the station in the Old Town of Vilnius. The meteogram (Figure 4) showed that meteorological conditions were exceptional in terms of wind speed (or humidity and atmospheric stability). Low wind speeds were also observed a week later, on 8 and 10 January, but there was no such increase in CO, PM<sub>10</sub>, and PM<sub>2.5</sub> (Figure 8). Given the average low air temperature and wind speed and high relative humidity, the meteorological conditions were favorable for the accumulation of air pollutants in the atmosphere. However, due to precipitation in the form of snow, the accumulation process might have been disturbed.

The fluctuations in the PM<sub>10</sub> concentration at the EPA sites and the mean concentration on New Year's Eve are shown in Figure 9. The maximum PM mass concentrations on New Year's Eve exceeded Q3 of the control period by 5 to 7 times, with the largest increase in the Old Town of Vilnius, where fireworks were most intense. The limits for PM<sub>2.5</sub> mass concentrations set by the WHO are as follows: 5 µg/m<sup>3</sup> annual mean and 15 µg/m<sup>3</sup> 24 h mean [53]. The mean values of PM<sub>10</sub> mass concentrations at the monitoring stations in Vilnius during the control period were close to or above the annual limit set by the WHO (15 µg/m<sup>3</sup>). The largest difference was observed at the Old Town station in the center of Vilnius (Figure 9), where the PM<sub>10</sub> concentration was about four times higher than the 24 h limit value (45 µg/m<sup>3</sup>) stated in the WHO Global Air Quality Guidelines. In general, the mean PM<sub>10</sub> concentration at all stations was close to or above the annual limit value set by the WHO. The PM<sub>2.5</sub> concentration was only monitored at the Žirmūnai station, which is located on a busy road. Here, the mean PM<sub>2.5</sub> mass concentration during the control period was three times higher than the annual limit set by the WHO, and the increase on New Year's Eve was 2.5 times the 24 h limit. However, this increase was observed before the fireworks, as the maximum PM<sub>1</sub> concentration was already reached at 23:00. Such tendencies were also studied by Pirker et al., 2022 [52]. The fireworks had no effect on PM<sub>1</sub> mass concentrations at the FTMC station (PM<sub>2.5</sub> and PM<sub>10</sub> data are not available here). However, increases in PM<sub>2.5</sub> and PM<sub>10</sub> mass concentrations were observed at the EPA stations (Figure 8), and this tendency was also observed by Khedr et al., 2022 [54]. The hourly PM<sub>2.5</sub> concentrations increased twofold (maximum at 2:00), and PM<sub>10</sub> concentrations increased by 1.4 to 2.6 times at the EPA stations compared to the hourly maximum after the fireworks (at 2:00) and the last hour before 1 January.

### 3.3. Changes in PM<sub>1</sub> Chemical Composition

For further analysis, only the night-time hours (from 9 p.m. to 6 a.m.) were analyzed. This time was chosen to exclude the evening and morning rush hours. For a typical night, the measurement data of a complete measurement campaign with the exception of New Year's Eve were averaged, and the same hours were selected for comparison with New Year's Eve.

During New Year's Eve, a significant alteration in PM<sub>1</sub> chemical composition and organic aerosol (OA) factors were observed (Figure 10, pie diagram in Figure 8). The typical chemical composition of outdoor PM<sub>1</sub> during the control period over night-time hours was dominated by OA (42%), followed by sulfate (23%), nitrate (16.5%), BC (9%), ammonium (8.5%) and trace element (1%) contributions. Meanwhile, the indoor air chemical composition during a typical night was close to the one in outdoor air (OA—47%, SO<sub>4</sub><sup>2-</sup>—21%, NO<sub>3</sub><sup>-</sup>—10%, BC—3%, trace elements—1%). During the event (from 9 p.m. to 6 a.m.), the contribution of OA to the total PM<sub>1</sub> increased from 43% to 70% and from 47% to 60% in outdoor and indoor air, respectively. In addition, a significant increase in BC mass contribution during New Year's Eve was observed in both outdoor (to 9%) and indoor (to 11%) air. These results are in agreement with other studies [55,56].

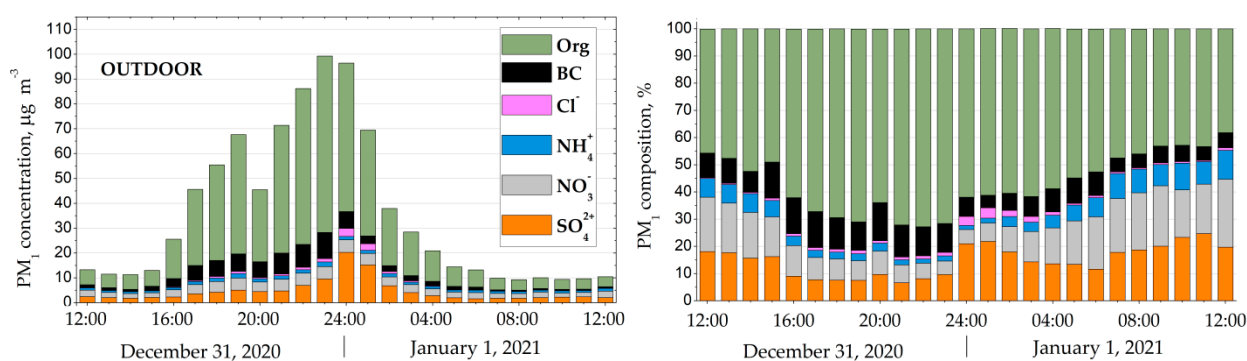


**Figure 10.** Hourly variation in PM<sub>1</sub> chemical composition and percentage on New Year's Eve.

Fireworks emissions caused a fourfold increase in Cl<sup>-</sup> concentration, with the maximum observed at 2:30 a.m. (up to 0.6 µg/m<sup>3</sup> in outdoor air and 0.05 µg/m<sup>3</sup> in indoor air, compared to a typical night: 0.1 µg/m<sup>3</sup> and 0.02 µg/m<sup>3</sup>, respectively). In addition, SO<sub>4</sub><sup>2-</sup> increased from 3.6 µg/m<sup>3</sup> and 0.2 µg/m<sup>3</sup> during a typical night to 4.7 µg/m<sup>3</sup> and 0.3 µg/m<sup>3</sup> during New Year's Eve (at 2:30 a.m.) in outdoor and indoor air, respectively (Figure 10). The NO<sub>3</sub><sup>-</sup> concentrations (4.0 µg/m<sup>3</sup> and 0.1 µg/m<sup>3</sup> in outdoor and indoor air, respectively) were 1.8 and 1.9 times higher compared to those during a typical night.

The concentrations of sulfate and chloride increased the most compared to the typical period as PM<sub>1</sub> compounds (Table 1). In contrast to BC and organics, the increase in these components was small before midnight and increased significantly by 2 and 2.5 times, respectively, after midnight. Therefore, this increase could be attributed to the fireworks.

This study showed a relatively good correlation up to 0.8 between the indoor and outdoor mass concentrations of PM<sub>1</sub> chemical components for the whole measurement campaign (Supplementary Materials Table S2), indicating a significant contribution of outdoor air pollution to indoor air due to the lower filtration factor of PM<sub>1</sub>. Research on the relationship between indoor and outdoor air quality indicates a demand for more efficient and improved ventilation and filtration systems that could detain air pollutants and help reduce the quantity of PM inside buildings during increased pollution events. Furthermore, Mendoza et al. [10] proved that outdoor air pollution is an important factor influencing indoor air quality—the infiltrated air pollutant highly depends on the particular pollution source.

### 3.4. BC Source Apportionment in Indoor/Outdoor Air

Figure 11 shows the variations in hourly averaged mass concentrations of BC from fossil fuel combustion (BC<sub>ff</sub>) and biomass burning (BC<sub>bb</sub>), as well as the contribution of source-specific BC components both outdoors and indoors. On New Year's Eve (between 6 p.m. and 6 a.m.), outdoor concentrations of BC<sub>ff</sub> and BC<sub>bb</sub> ranged from 1.38 to 11.04 µg/m<sup>3</sup> (average 4.93 ± 3.72 µg/m<sup>3</sup>) and 0.42 to 2.80 µg/m<sup>3</sup> (average 1.55 ± 0.9 µg/m<sup>3</sup>), respectively. The contribution of BC<sub>bb</sub> to the total BC was 24%. The indoor concentration of BC<sub>ff</sub> and BC<sub>bb</sub> varied in a range of 0.04–0.35 µg/m<sup>3</sup> (average 0.18 ± 0.12 µg/m<sup>3</sup>) and

0.01–0.32  $\mu\text{g}/\text{m}^3$  (average  $0.13 \pm 0.12 \mu\text{g}/\text{m}^3$ ), respectively. During the event, the proportion of  $\text{BC}_{\text{bb}}$  in indoor/outdoor air was about 13%.

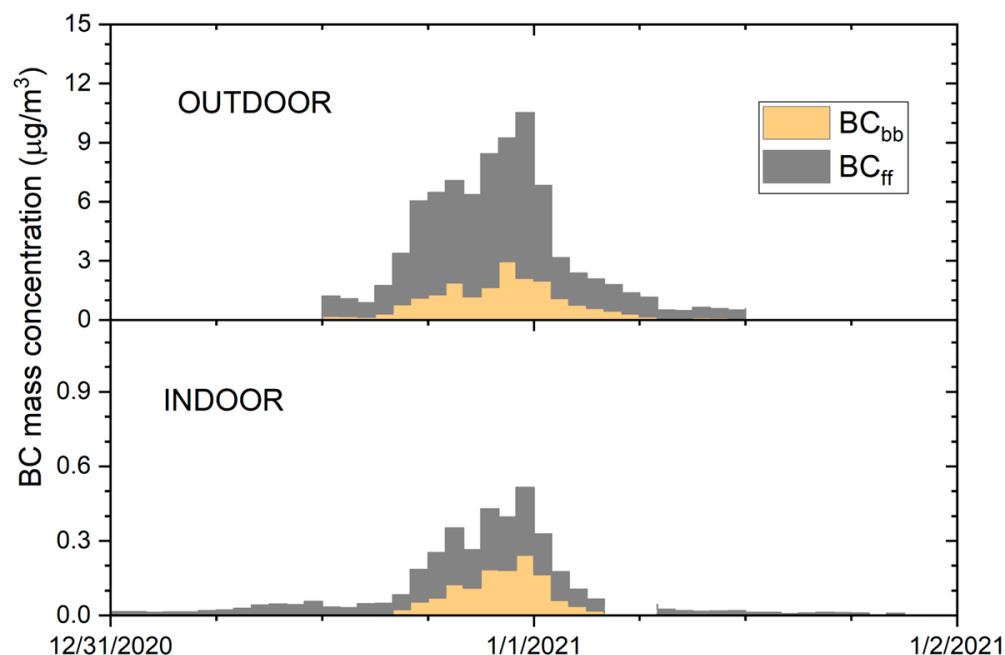


**Figure 11.** Apportionment of BC outdoors and indoors on New Year's Eve and afterwards (stacked diagram).

These results were compared with BC values on a typical night.  $\text{BC}_{\text{bb}}$  mass concentrations were 11.2 and 26.5 times higher in outdoor and indoor air, respectively, during the event. Meanwhile, the  $\text{BC}_{\text{ff}}$  concentration was found to be 10.1 (in outdoor air) and 11.1 (in indoor air) times higher during the event compared to a typical night.

Measured outdoor BC concentrations and source distributions were similar or lower in Vilnius than in other European sites.  $\text{BC}_{\text{bb}}/\text{BC}$  was similar in both indoor and outdoor air, suggesting that the distribution of BC sources was not altered by transport from outdoors to indoors.

### 3.5. OA Source Apportionment in Indoor/Outdoor Air

For further analysis, a PMF solution for assigning OA to different sources was investigated (Figure 12). Compared to the typical values, on New Year's Eve, the mass concentration of biomass-burning organic aerosol (BBOA) increased 9.8 times to  $32.8 \mu\text{g}/\text{m}^3$  in outdoor air and 5.2 times to  $1.2 \mu\text{g}/\text{m}^3$  in indoor air. Similar levels were observed for hydrocarbon-like organic aerosol (HOA), which was 9.2 times (up to  $14.3 \mu\text{g}/\text{m}^3$ ) and 6.6 times (up to  $1.0 \mu\text{g}/\text{m}^3$ ) higher than the average night-time levels in outdoor and indoor air, respectively.

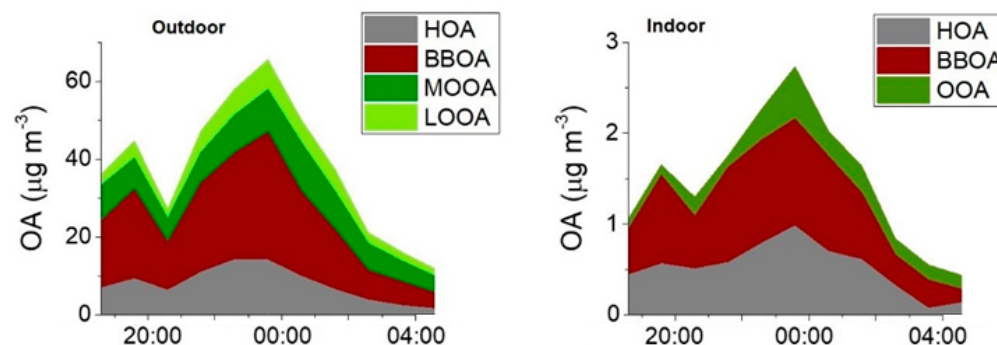


**Figure 12.** Time series of OA sources in outdoor (left) and indoor (right) air during New Year's Eve (MOOA stands for 'More Oxidized Oxygenated Organic Aerosol' and LOOA for 'Less Oxygenated Organic Aerosol').

While HOA was likely linked to increased traffic during the event, BBOA could be associated with residential heating and additional burning processes associated with fireworks. In order to confirm this hypothesis, triangle plots were created (Figure 13). The triangle plot demonstrates space of  $m/z$  44 and 43 normalized to OA ( $f_{44}$  and  $f_{43}$ , respectively).  $m/z$  44 and 43 are prominent OA peaks representing different oxygen-containing groups that provide some insights into atmospheric OA evolution. As shown in Figure 13, the highest BBOA mass concentrations in outdoor air occurred together with the lowest  $f_{44}$  and  $f_{43}$  values. This result suggests that elevated BBOA levels were not due to heating-related OA, but rather, were freshly emitted during the event. Interestingly, a similar pattern was observed indoors, confirming the importance of primary outdoor OA to indoor air quality. Minor differences in the distribution of data points within the triangular plot in indoor air could be associated with increased uncertainty due to the low mass concentration values.

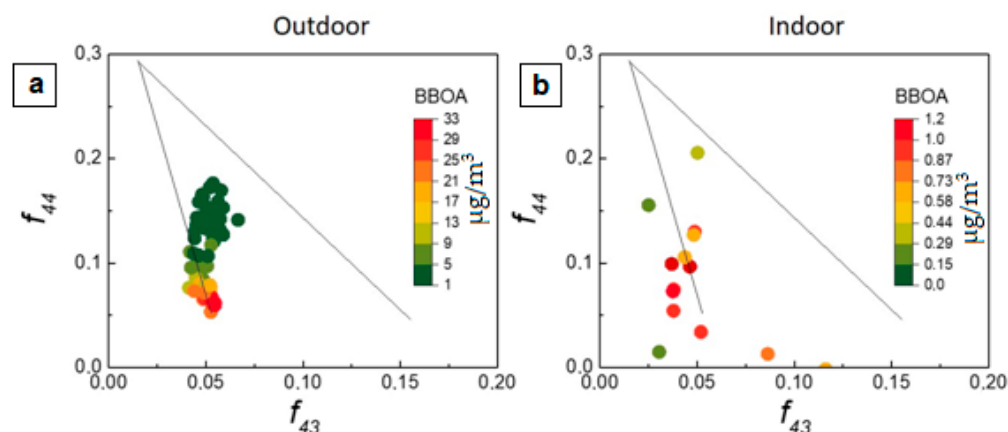


**Figure 13.** Triangular plots for outdoor air (a) and indoor air (b) for OA during the event. Gray lines are added to define the triangular  $f_{44}$  and  $f_{43}$  space. Color indicates the BBOA mass concentration. Due to the low concentrations in the indoor air (close to signal to noise ratio), several data points were removed from the indoor air plot.

After applying the ISSOROPIA model to the aerosol chemical composition data, the mass concentration of  $\text{Na}^+$  was evaluated for both indoor and outdoor air. Figure 14 shows that the  $\text{Na}^+$  mass concentration increased significantly during the event in both outdoor and indoor air, reaching  $11.8 \mu\text{g}/\text{m}^3$  and  $0.2 \mu\text{g}/\text{m}^3$ , respectively. These values were 4.8 times (in outdoor air) and 2.5 times (in indoor air) higher than typical night-time levels.

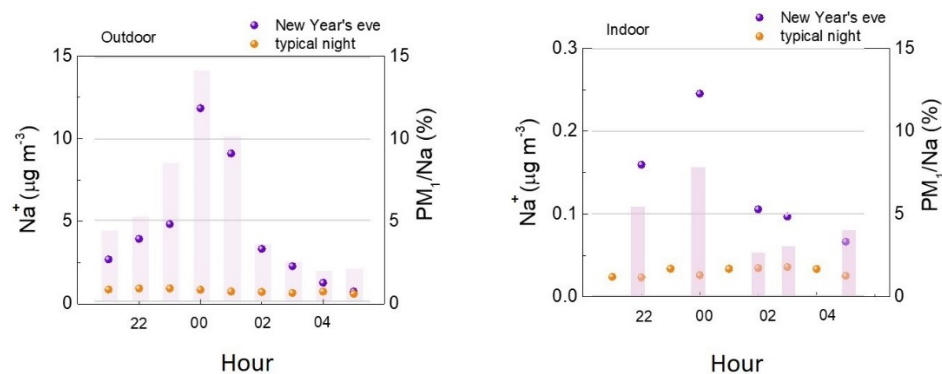


**Figure 14.** Time series of Na<sup>+</sup> levels in outdoor (A) and indoor (B) air on New Year's Eve (purple) and typical night (orange). The columns show the Na<sup>+</sup> input to PM<sub>1</sub>. This alteration in Na<sup>+</sup> levels was somewhat expected due to the important role of sodium salts in fireworks-related chemistry [53]. Yet, the enrichment of Na<sup>+</sup> levels in indoor air confirms a strong influence of fireworks' chemistry on indoor air quality.

#### 4. Conclusions

The high levels of air pollution observed on the night of 31 December 2020 to 1 January 2021 were caused by weather conditions and fireworks in the Vilnius urban background site. The meteorological conditions on New Year's Eve were favorable for the accumulation of particulate matter in the atmosphere, given the stability of the atmosphere (the low depth of the planetary boundary layer), the relatively low air temperature, and the low wind speed. In this study, we have highlighted a situation where extremely foggy meteorological conditions coincided with intense anthropogenic emissions, including fireworks.

Aerosol source apportionment was performed using PMF to analyze the contributions of fireworks to PM<sub>1</sub> in outdoor and indoor air. The wind speed reached its lowest values before midnight. Due to household heating and intense traffic emissions, the mass concentrations of both BC<sub>bb</sub> and BC<sub>ff</sub> were more than 10 times higher during the evening compared to a typical night. During New Year's Eve, organic compounds dominated (70%) the outdoor and indoor (60%) air. However, biomass-burning organic aerosols during the event increased 9.8 times in outdoor air, reaching 32.8 µg/m<sup>3</sup> and 5.2 times in indoor air up to 1.2 µg/m<sup>3</sup> compared to the typical night-time. Comparable levels were recorded for hydrocarbon-like organic aerosol which was 9.2 times and 6.6 times higher than the average night-time levels in outdoor and indoor air, respectively. Moreover, the result of the triangle plot suggests that increased levels of biomass-burning organic aerosols were freshly emitted during New Year's night. Also, a similar tendency was observed indoors.

The contribution of fireworks to the observed increase in hourly PM<sub>2.5</sub> concentrations after midnight on New Year's Eve was about 50% (of the maximum value at 2:30 a.m.), and to PM<sub>10</sub> concentrations, from 30% to 60% at EPA stations in Vilnius (of the maximum value at 2:30 a.m.). The increase in PM<sub>1</sub> compounds such as sulfate and chloride concentrations, reflected in the change in the percentage distribution of contributions after midnight, could also have been due to the fireworks. Na<sup>+</sup> mass concentrations increased significantly after the New Year's Eve fireworks in both outdoor and indoor air, with values 4.8 times (in outdoor air) and 2.5 times (in indoor air) higher than typical winter night-time values.

We would like to point out the limitations of our study. First of all, only one air quality monitoring site was used for this work. However, in order to have a broader and deeper understanding of the air quality situation in the urban background site during the New Year event, we used the air quality monitoring stations belonging to the Environmental Protection Agency (AAA), which measure PM<sub>2.5</sub>, PM<sub>10</sub>, NO<sub>2</sub>, and CO mass concentrations and meteorological parameters. Secondly, the higher time resolutions of the devices used in this study prevented the real-time monitoring of the dynamics of the concentration level of particulate matter, their components, and gases in the city. Nevertheless, each method has

its own restrictions and capacities; therefore, it is most valuable to use different methods and devices complementarily.

**Supplementary Materials:** The following supporting information can be downloaded at <https://www.mdpi.com/article/10.3390/urbansci8020054/s1>: Figure S1: PMF solution profiles and time series; Table S1:  $\theta$  values for different indoor and outdoor factors; Table S2: Correlations between the same aerosol chemical component or factor in outdoor versus indoor air. References [57–61] are cited in the file of Supplementary Materials.

**Author Contributions:** Conceptualization, S.B. and L.D.; data curation, J.P. and A.M.; formal analysis, S.B. and L.D.; methodology, J.P., A.M. and A.K.; resources, S.B.; software, J.P. and A.K.; supervision, S.B.; validation, L.D.; investigation, J.P. and A.K.; visualization, J.P., A.K. and A.M.; writing—original draft preparation, A.K., L.D. and J.P.; writing—review and editing, L.D. and J.P.; funding acquisition, S.B. All authors have read and agreed to the published version of the manuscript.

**Funding:** This research received no external funding.

**Institutional Review Board Statement:** Not applicable.

**Informed Consent Statement:** Not applicable.

**Data Availability Statement:** The data presented in this study are available upon request from the corresponding author.

**Acknowledgments:** Air pollution data were provided by the Environmental Protection Agency of Lithuania.

**Conflicts of Interest:** The authors declare no conflicts of interest.

## References

1. Singh, A.; Pant, P.; Pope, F.D. Air Quality during and after Festivals: Aerosol Concentrations, Composition and Health Effects. *Atmos. Res.* **2019**, *227*, 220–232. [CrossRef]
2. Rose Lorenzo, G.; Angela Bañaga, P.; Obiminda Cambaliza, M.; Templonuevo Cruz, M.; Azadiaghdam, M.; Arellano, A.; Betito, G.; Braun, R.; Corral, A.F.; Dadashazar, H.; et al. Measurement Report: Firework Impacts on Air Quality in Metro Manila, Philippines, during the 2019 New Year Revelry. *Atmos. Chem. Phys.* **2021**, *21*, 6155–6173. [CrossRef]
3. Rindelaub, J.D.; Davy, P.K.; Talbot, N.; Pattinson, W.; Miskelly, G.M. The Contribution of Commercial Fireworks to Both Local and Personal Air Quality in Auckland, New Zealand. *Environ. Sci. Pollut. Res. Int.* **2021**, *28*, 21650–21660. [CrossRef] [PubMed]
4. World Health Organization. *Ambient Air Pollution: A Global Assessment of Exposure and Burden of Disease*; World Health Organization: Geneva, Switzerland, 2016.
5. Bach, W.; Daniels, A.; Dickinson, L.E.; Hertlein, F.; Morrows, J.; Margolis, S.V.; Dinh, V.D. Fireworks Pollution and Health. *Int. J. Environ. Stud.* **1975**, *7*, 183–192. [CrossRef]
6. Achilleos, S.; Kioumourtzoglou, M.A.; Wu, C.D.; Schwartz, J.D.; Koutrakis, P.; Papatheodorou, S.I. Acute Effects of Fine Particulate Matter Constituents on Mortality: A Systematic Review and Meta-Regression Analysis. *Environ. Int.* **2017**, *109*, 89–100. [CrossRef]
7. Hoyos, C.D.; Herrera-Mejía, L.; Roldán-Henao, N.; Isaza, A. Effects of Fireworks on Particulate Matter Concentration in a Narrow Valley: The Case of the Medellín Metropolitan Area. *Environ. Monit. Assess.* **2020**, *192*, 6. [CrossRef]
8. Yao, L.; Wang, D.; Fu, Q.; Qiao, L.; Wang, H.; Li, L.; Sun, W.; Li, Q.; Wang, L.; Yang, X.; et al. The Effects of Firework Regulation on Air Quality and Public Health during the Chinese Spring Festival from 2013 to 2017 in a Chinese Megacity. *Environ. Int.* **2019**, *126*, 96–106. [CrossRef] [PubMed]
9. Chen, S.; Jiang, L.; Liu, W.; Song, H. Fireworks Regulation, Air Pollution, and Public Health: Evidence from China. *Reg. Sci. Urban. Econ.* **2022**, *92*, 103722. [CrossRef]
10. Mendoza, D.L.; Benney, T.M.; Boll, S. Long-Term Analysis of the Relationships between Indoor and Outdoor Fine Particulate Pollution: A Case Study Using Research Grade Sensors. *Sci. Total Environ.* **2021**, *776*, 145778. [CrossRef]
11. Settimo, G.; D’Alessandro, D. European Community Guidelines and Standards in Indoor Air Quality: What Proposals for Italy. *Epidemiol. Prev.* **2014**, *38* (Suppl. 2), 36–41.
12. World Health Organization. Household Air Pollution and Health. Available online: <https://www.who.int/news-room/fact-sheets/detail/household-air-pollution-and-health> (accessed on 27 December 2023).
13. Moreno, T.; Querol, X.; Alastuey, A.; Amato, F.; Pey, J.; Pandolfi, M.; Kuenzli, N.; Bouso, L.; Rivera, M.; Gibbons, W. Effect of Fireworks Events on Urban Background Trace Metal Aerosol Concentrations: Is the Cocktail Worth the Show? *J. Hazard. Mater.* **2010**, *183*, 945–949. [CrossRef] [PubMed]
14. Zhang, R.; Wang, G.; Guo, S.; Zamora, M.L.; Ying, Q.; Lin, Y.; Wang, W.; Hu, M.; Wang, Y. Formation of Urban Fine Particulate Matter. *Chem. Rev.* **2015**, *115*, 3803–3855. [CrossRef] [PubMed]

15. Barman, S.C.; Singh, R.; Negi, M.P.S.; Bhargava, S.K. Ambient Air Quality of Lucknow City (India) during Use of Fireworks on Diwali Festival. *Environ. Monit. Assess.* **2008**, *137*, 495–504. [[CrossRef](#)] [[PubMed](#)]
16. Gonzalez, A.; Boies, A.; Swanson, J.; Kittelson, D. Measuring the Effect of Fireworks on Air Quality in Minneapolis, Minnesota. *SN Appl. Sci.* **2022**, *4*, 142. [[CrossRef](#)]
17. Lin, C.C. A Review of the Impact of Fireworks on Particulate Matter in Ambient Air. *J. Air Waste Manag. Assoc.* **2016**, *66*, 1171–1182. [[CrossRef](#)]
18. Seidel, D.J.; Birnbaum, A.N. Effects of Independence Day Fireworks on Atmospheric Concentrations of Particulate Matter in the United States. *Atmos. Environ.* **2015**, *115*, 192–198. [[CrossRef](#)]
19. Joshi, M.; Nakhwa, A.; Khandare, P.; Khan, A.; Mariam; Sapra, B.K. Simultaneous Measurements of Mass, Chemical Compositional and Number Characteristics of Aerosol Particles Emitted during Fireworks. *Atmos. Environ.* **2019**, *217*, 116925. [[CrossRef](#)]
20. Moreno, T.; Querol, X.; Alastuey, A.; Cruz Minguillón, M.; Pey, J.; Rodriguez, S.; Vicente Miró, J.; Felis, C.; Gibbons, W. Recreational Atmospheric Pollution Episodes: Inhalable Metalliferous Particles from Firework Displays. *Atmos. Environ.* **2007**, *41*, 913–922. [[CrossRef](#)]
21. Sarkar, S.; Khillare, P.S.; Jyethi, D.S.; Hasan, A.; Parween, M. Chemical Speciation of Respirable Suspended Particulate Matter during a Major Firework Festival in India. *J. Hazard. Mater.* **2010**, *184*, 321–330. [[CrossRef](#)]
22. Pathak, B.; Biswas, J.; Bharali, C.; Bhuyan, P.K. Short Term Introduction of Pollutants into the Atmosphere at a Location in the Brahmaputra Basin: A Case Study. *Atmos. Pollut. Res.* **2015**, *6*, 220–229. [[CrossRef](#)]
23. Joly, A.; Smargiassi, A.; Kosatsky, T.; Fournier, M.; Dabek-Zlotorzynska, E.; Celis, V.; Mathieu, D.; Servranckx, R.; D'amours, R.; Malo, A.; et al. Characterisation of Particulate Exposure during Fireworks Displays. *Atmos. Environ.* **2010**, *44*, 4325–4329. [[CrossRef](#)]
24. Wehner, B.; Wiedensohler, A.; Heintzenberg, J. Submicrometer Aerosol Size Distributions and Mass Concentration of the Millennium Fireworks 2000 in Leipzig, Germany. *J. Aerosol Sci.* **2000**, *31*, 1489–1493. [[CrossRef](#)]
25. Joshi, M.; Khan, A.; Anand, S.; Sapra, B.K. Size Evolution of Ultrafine Particles: Differential Signatures of Normal and Episodic Events. *Environ. Pollut.* **2016**, *208*, 354–360. [[CrossRef](#)]
26. Hussein, T.; Dal Maso, M.; Petaja, T.; Paatero, P.; Aalto, P.P.; Haemerli, K.; Kulmala, M.; Koponen, I.K. Evaluation of an Automatic Algorithm for Fitting the Particle Number Size Distributions. *Boreal. Environ. Res.* **2005**, *10*, 337.
27. Singh, D.P.; Gadi, R.; Mandal, T.K.; Dixit, C.K.; Singh, K.; Saud, T.; Singh, N.; Gupta, P.K. Study of Temporal Variation in Ambient Air Quality during Diwali Festival in India. *Environ. Monit. Assess.* **2010**, *169*, 1–13. [[CrossRef](#)]
28. Lai, Y.; Brimblecombe, P. Changes in Air Pollution and Attitude to Fireworks in Beijing. *Atmos. Environ.* **2020**, *231*, 117549. [[CrossRef](#)]
29. Pang, N.; Gao, J.; Zhao, P.; Wang, Y.; Xu, Z.; Chai, F. The Impact of Fireworks Control on Air Quality in Four Northern Chinese Cities during the Spring Festival. *Atmos. Environ.* **2021**, *244*, 117958. [[CrossRef](#)]
30. Zhang, Y.; Favez, O.; Petit, J.-E.; Canonaco, F.; Truong, F.; Bonnaire, N.; Crenn, V.; Amodeo, T.; Prévôt, A.S.H.; Sciare, J.; et al. Six-Year Source Apportionment of Submicron Organic Aerosols from near-Continuous Highly Time-Resolved Measurements at SIRTIA (Paris Area, France). *Atmos. Chem. Phys.* **2019**, *19*, 14755–14776. [[CrossRef](#)]
31. Dall'Osto, M.; Beddows, D.C.S.; McGillicuddy, E.J.; Esser-Gietl, J.K.; Harrison, R.M.; Wenger, J.C. On the Simultaneous Deployment of Two Single-Particle Mass Spectrometers at an Urban Background and a Roadside Site during SAPUSS. *Atmos. Chem. Phys.* **2016**, *16*, 9693–9710. [[CrossRef](#)]
32. Moffet, R.C.; de Foy, B.; Molina, L.T.; Molina, M.J.; Prather, K.A. Measurement of Ambient Aerosols in Northern Mexico City by Single Particle Mass Spectrometry. *Atmos. Chem. Phys.* **2007**, *8*, 4499–4516. [[CrossRef](#)]
33. Xu, J.; Tian, Y.; Cheng, C.; Wang, C.; Lin, Q.; Li, M.; Wang, X.; Shi, G. Characteristics and Source Apportionment of Ambient Single Particles in Tianjin, China: The Close Association between Oxalic Acid and Biomass Burning. *Atmos. Res.* **2020**, *237*, 104843. [[CrossRef](#)]
34. Vecchi, R.; Bernardoni, V.; Cricchio, D.; D'Alessandro, A.; Fermo, P.; Lucarelli, F.; Nava, S.; Piazzalunga, A.; Valli, G. The Impact of Fireworks on Airborne Particles. *Atmos. Environ.* **2008**, *42*, 1121–1132. [[CrossRef](#)]
35. Tsai, H.-H.; Chien, L.-H.; Yuan, C.; Lin, Y.-C.; Jen, Y.-H.; Ie, I.-R. Influences of Fireworks on Chemical Characteristics of Atmospheric Fine and Coarse Particles during Taiwan's Lantern Festival. *Atmos. Environ.* **2012**, *62*, 256–264. [[CrossRef](#)]
36. Center for Physical Sciences and Technology (FTMC). Available online: <https://www.ftmc.lt/en/> (accessed on 1 July 2021).
37. DIN EN ISO 16890. Available online: <https://airfiltration.mann-hummel.com/en/insights/filtration/filter-classification/din-en-iso-16890.html> (accessed on 27 December 2023).
38. Sandradewi, J.; Prévôt, A.S.H.; Weingartner, E.; Schmidhauser, R.; Gysel, M.; Baltensperger, U. A Study of Wood Burning and Traffic Aerosols in an Alpine Valley Using a Multi-Wavelength Aethalometer. *Atmos. Environ.* **2008**, *42*, 101–112. [[CrossRef](#)]
39. Minderytė, A.; Pauraitė, J.; Dudoitis, V.; Plauškaitė, K.; Kilikevičius, A.; Matijošius, J.; Rimkus, A.; Kilikevičienė, K.; Vainorius, D.; Byčėnienė, S. Carbonaceous Aerosol Source Apportionment and Assessment of Transport-Related Pollution. *Atmos. Environ.* **2022**, *279*, 119043. [[CrossRef](#)]
40. Xu, J.; Shi, J.; Zhang, Q.; Ge, X.; Canonaco, F.; Prévôt, A.S.H.; Vonwiller, M.; Szidat, S.; Ge, J.; Ma, J.; et al. Wintertime Organic and Inorganic Aerosols in Lanzhou, China: Sources, Processes, and Comparison with the Results during Summer. *Atmos. Chem. Phys.* **2016**, *16*, 14937–14957. [[CrossRef](#)]

41. Garbarienė, I.; Pauraitė, J.; Pashneva, D.; Minderytė, A.; Sarka, K.; Dudoitis, V.; Davulienė, L.; Gaspariūnas, M.; Kovalevskij, V.; Lingis, D.; et al. Indoor-Outdoor Relationship of Submicron Particulate Matter in Mechanically Ventilated Building: Chemical Composition, Sources and Infiltration Factor. *BUILD. Environ.* **2022**, *222*, 109429. [[CrossRef](#)]
42. Fountoukis, C.; Nenes, A. ISORROPIA II: A computationally efficient thermodynamic equilibrium model for  $K^+Ca^{2+}Mg^{2+}NH_4^+Na^+SO_4^{2-}NO_3^-Cl^-H_2O$  aerosols. *Atmos. Chem. Phys.* **2007**, *7*, 4639–4659. [[CrossRef](#)]
43. Rolph, G.; Stein, A.; Stunder, B. Real-Time Environmental Applications and Display System: READY. *Environ. Model. Softw.* **2017**, *95*, 210–228. [[CrossRef](#)]
44. Stein, A.F.; Draxler, R.R.; Rolph, G.D.; Stunder, B.J.B.; Cohen, M.D.; Ngan, F. NOAA's HYSPLIT Atmospheric Transport and Dispersion Modeling System. *Bull. Am. Meteorol. Soc.* **2015**, *96*, 2059–2077. [[CrossRef](#)]
45. Heffter, J.L.; Secretary, M.B.; Byrne, J.V.; Ludwig Director, G.H. *Branching Atmospheric Trajectory (Bat) Model*; NOAA Technical Memorandum ERL ARL-121; United States Department of Commerce: Washington, DC, USA, 1983.
46. Ji, D.; Wang, Y.; Wang, L.; Chen, L.; Hu, B.; Tang, G.; Xin, J.; Song, T.; Wen, T.; Sun, Y.; et al. Analysis of Heavy Pollution Episodes in Selected Cities of Northern China. *Atmos. Environ.* **2012**, *50*, 338–348. [[CrossRef](#)]
47. Olofson, K.F.G.; Andersson, P.U.; Hallquist, M.; Ljungström, E.; Tang, L.; Chen, D.; Pettersson, J.B.C. Urban Aerosol Evolution and Particle Formation during Wintertime Temperature Inversions. *Atmos. Environ.* **2009**, *43*, 340–346. [[CrossRef](#)]
48. Safai, P.D.; Ghude, S.; Pithani, P.; Varpe, S.; Kulkarni, R.; Todekar, K.; Tiwari, S.; Chate, D.M.; Prabhakaran, T.; Jenamani, R.K.; et al. Two-Way Relationship between Aerosols and Fog: A Case Study at IGI Airport, New Delhi. *Aerosol Air Qual. Res.* **2019**, *19*, 71–79. [[CrossRef](#)]
49. Phung Ngoc, B.A.; Delbarre, H.; Deboudt, K.; Dieudonné, E.; Nguyen Tran, D.; Le Thanh, S.; Pelon, J.; Ravetta, F. Key Factors Explaining Severe Air Pollution Episodes in Hanoi during 2019 Winter Season. *Atmos. Pollut. Res.* **2021**, *12*, 101068. [[CrossRef](#)]
50. Seinfeld, J.H.; Pandis, S.N. *Atmospheric Chemistry and Physics. From Air Pollution to Climate Change*, 2nd ed.; Wiley-Interscience: Hoboken, NJ, USA, 2006.
51. Quan, J.; Gao, Y.; Zhang, Q.; Tie, X.; Cao, J.; Han, S.; Meng, J.; Chen, P.; Zhao, D. Evolution of Planetary Boundary Layer under Different Weather Conditions, and Its Impact on Aerosol Concentrations. *Particuology* **2013**, *11*, 34–40. [[CrossRef](#)]
52. Pirker, L.; Velkavrh, Ž.; Osíte, A.; Drinovec, L.; Močnik, G.; Remškar, M. Fireworks—A Source of Nanoparticles, PM<sub>2.5</sub>, PM<sub>10</sub>, and Carbonaceous Aerosols. *Air Qual. Atmos. Health* **2022**, *15*, 1275–1286. [[CrossRef](#)]
53. World Health Organization. *WHO Global Air Quality Guidelines: Particulate Matter (PM<sub>2.5</sub> and PM<sub>10</sub>), Ozone, Nitrogen Dioxide, Sulfur Dioxide and Carbon Monoxide*; World Health Organization: Geneva, Switzerland, 2021.
54. Khedr, M.; Liu, X.; Hadiatullah, H.; Orasche, J.; Zhang, X.; Cyrus, J.; Michalke, B.; Zimmermann, R.; Schnelle-Kreis, J. Influence of New Year's Fireworks on Air Quality—A Case Study from 2010 to 2021 in Augsburg, Germany. *Atmos. Pollut. Res.* **2022**, *13*, 101341. [[CrossRef](#)]
55. Zhang, J.; Lance, S.; Freedman, J.M.; Sun, Y.; Crandall, B.A.; Wei, X.; Schwab, J.J. Detailed Measurements of Submicron Particles from an Independence Day Fireworks Event in Albany, New York Using HR-ToF-AMS. *ACS Earth Space Chem.* **2019**, *3*, 1451–1459. [[CrossRef](#)]
56. Retama, A.; Neria-Hernández, A.; Jaimes-Palomera, M.; Rivera-Hernández, O.; Sánchez-Rodríguez, M.; López-Medina, A.; Velasco, E. Fireworks: A Major Source of Inorganic and Organic Aerosols during Christmas and New Year in Mexico City. *Atmos. Environ. X* **2019**, *2*, 100013. [[CrossRef](#)]
57. Paglione, M.; Gilardoni, S.; Rinaldi, M.; Decesari, S.; Zanca, N.; Sandrini, S.; Giulianelli, L.; Bacco, D.; Ferrari, S.; Poluzzi, V.; et al. The impact of biomass burning and aqueous-phase processing on air quality: A multi-year source apportionment study in the Po Valley, Italy. *Atmos. Chem. Phys.* **2020**, *20*, 1233–1254. [[CrossRef](#)]
58. Paatero, P. A weighted non-negative least squares algorithm for three-way "PARAFAC" factor analysis. *Chemom. Intell. Lab. Syst.* **1997**, *38*, 223–242. [[CrossRef](#)]
59. Canonaco, F.; Crippa, M.; Slowik, J.G.; Baltensperger, U.; Prévôt, A.S.H. SoFi, an IGOR-based interface for the efficient use of the generalized multilinear engine (ME-2) for the source apportionment: ME-2 application to aerosol mass spectrometer data. *Atmos. Meas. Tech.* **2013**, *6*, 3649–3661. [[CrossRef](#)]
60. Cubison, M.J.; Ortega, A.M.; Hayes, P.L.; Farmer, D.K.; Day, D.; Lechner, M.J.; Brune, W.H.; Apel, E.; Diskin, G.S.; Fisher, J.A.; et al. Effects of aging on organic aerosol from open biomass burning smoke in aircraft and laboratory studies. *Atmos. Chem. Phys.* **2011**, *11*, 12049–12064. [[CrossRef](#)]
61. Kostenidou, E.; Lee, B.-H.; Engelhart, G.J.; Pierce, J.R.; Pandis, S.N. Mass Spectra Deconvolution of Low, Medium, and High Volatility Biogenic Secondary Organic Aerosol. *Environ. Sci. Technol.* **2009**, *43*, 4884–4889. [[CrossRef](#)] [[PubMed](#)]

**Disclaimer/Publisher's Note:** The statements, opinions and data contained in all publications are solely those of the individual author(s) and contributor(s) and not of MDPI and/or the editor(s). MDPI and/or the editor(s) disclaim responsibility for any injury to people or property resulting from any ideas, methods, instructions or products referred to in the content.